



UNIVERSITI PUTRA MALAYSIA

**EXPERIMENTAL AND FINITE ELEMENT ANALYSES OF
CORRUGATED WEB STEEL BEAMS SUBJECTED TO BENDING
LOADS**

CHAN CHEE LEONG

FK 2002 57

**EXPERIMENTAL AND FINITE ELEMENT ANALYSES OF
CORRUGATED WEB STEEL BEAMS SUBJECTED TO BENDING LOADS**

By

CHAN CHEE LEONG

**Thesis Submitted to the School of Graduate Studies, Universiti Putra Malaysia,
in Fulfilment of the Requirement for the Degree of Master of Science**

September 2002



Abstract of thesis presented to the Senate of Universiti Putra Malaysia in fulfilment of the requirements for the degree of Master of Science

**EXPERIMENTAL AND FINITE ELEMENT ANALYSES OF
CORRUGATED WEB STEEL BEAMS SUBJECTED TO BENDING LOADS**

By

CHAN CHEE LEONG

September 2002

Chairman : Associate Professor Yousif A. Khalid, Ph.D.

Faculty : Engineering

The behaviour of beams with corrugated web has been investigated throughout this study. They are commonly used in structural steel works to enhance the moment-carrying capability and weight reduction. Experimental tests and finite element analysis were conducted on beams with plane web (PW), horizontally corrugated (HC) and vertically corrugated (VC) webs.

Throughout the experimental tests, semicircular shape corrugation of 22.5 mm mean radius and 4.0 mm thickness was used. Two cases were considered for the HC beams, one arc (HC1) and two arcs (HC2) corrugation, while semicircular wholly corrugated was used for the VC type beams. All specimens were fabricated using tubes and flat plates of mild steel material (AISI 1020). The Instron testing machine was used for the three-point bending tests where three tests for each case have been carried out to obtain the load-displacement relations. The plane web I-section beams

with the mass per unit length value of $19.3 \text{ (kgm}^{-1}\text{)}$ was also tested to act as the benchmark result.

In the analytical work, finite element models were generated and analysed by using LUSAS software. The material datasets were defined based on the actual stress-strain data obtained from the tensile tests. A series of elastic-plastic nonlinear analysis were carried out with the boundary settings similar to the experiment setup. Three corrugation radii of 22.50 mm, 33.75 mm and 67.50 mm were considered for the HC beams while five radii, in the range of 11.25 mm to 33.75 mm for the VC beams.

From the results obtained, the VC beams has yield loads of 60.621 kN to 73.308 kN or 13.3% to 32.8% higher than the welded plane web beams and 1.32-1.89 times and 1.56-3.26 times higher compared to the HC1 and HC2 beams respectively. The yield load increases as the larger size of radius was used, which is true for the sizes taken in this study. Moreover, as much as 13.6% of reduction in weight was achieved for the VC beams at the largest value of corrugation radius. A good agreement was found between the experimental and finite element analysis results where the percentage difference obtained was 7.28% to 28.37%.

Abstrak tesis yang dikemukakan kepada Senat Universiti Putra Malaysia sebagai memenuhi keperluan untuk ijazah Master Sains

**EKSPERIMEN DAN ANALISIS UNSUR TERHINGGA ALANG BESI
BERALUN DIKENAKAN BEBAN MEMBENGGOK**

By

CHAN CHEE LEONG

September 2002

Pengerusi : Profesor Madya Yousif A. Khalid, Ph.D.

Fakulti : Kejuruteraan

Kajian ke atas kelakuan alang beralun telah dijalankan. Ia biasanya digunakan untuk kerja-kerja melibatkan struktur besi dalam mempertingkatkan keupayaan menanggung beban momen dan mengurangkan berat struktur. Alang dengan bentuk rim tengah yang berbeza iaitu datar (PW), beralun melintang (HC) dan beralun menegak telah dikaji secara ujikaji dan analisis unsur terhingga.

Alunan berbentuk separuh bulatan dengan jejari min 22.5 mm dan tebal 4.0 mm digunakan dalam ujikaji. Bagi alang jenis HC, dua bentuk alunan dikaji iaitu satu lengkungan (HC1) dan dua lengkungan (HC2) dan alunan berbentuk separuh bulatan beralun menyeluruh bagi alang jenis VC. Semua spesimen dibikin dengan menggunakan bahan besi lembut (AISI 1020). Tiga ujian lenturan tiga-pin dijalankan ke atas setiap jenis alang dengan menggunakan mesin Instron untuk mendapatkan perkaitan di antara beban-sesaran. Alang biasa yang berbentuk I dengan rim tengah

yang rata juga diuji sebagai ujian kawalan. Berat semeter alang yang diuji ialah 19.3 kgm^{-1} .

Dalam kajian secara analitikal, model unsur terhingga dihasilkan dan diuji di bawah kesan lenturan tiga-pin dengan menggunakan perisian LUSAS. Sifat mekanikal bahan ditakrifkan daripada tegasan-terikan sebenar yang diperolehi dalam ujian ketegangan. Analisis-analisis tidak linear yang diprogramkan menyerupai keadaan dan susunan eksperimen telah dijalankan. Sebanyak tiga saiz jejari alunan digunakan bagi alang jenis HC iaitu 22.50 mm, 33.75 mm dan 67.50 mm, manakala lima saiz dalam lingkungan 11.25 mm hingga 33.75 mm bagi alang jenis VC.

Daripada keputusan yang diperolehi, alang jenis VC mempunyai nilai beban alah sebanyak 60.621kN hingga 73.308 kN atau 13.3% hingga 32.8% melebihi alang jenis PW yang dikimpal serta 1.32-1.89 dan 1.56-3.26 kali ganda nilai beban alah alang jenis HC1 dan HC2 masing-masing. Dengan menggunakan saiz jejari alunan yang besar, peningkatan dalam beban alah yang lebih ketara akan diperolehi. Tambahan pula, penurunan berat sebanyak 13.6% bagi alang jenis VC akan dicapai jika maksimum saiz jejari alunan digunakan. Perbandingan di antara keputusan eksperimen dan analisis unsur terhingga adalah memuaskan dengan peratus perbezaan yang diperolehi sebanyak 7.28% hingga 28.37%.

ACKNOWLEDGEMENTS

I would like to express my sincere gratitude to all my supervisors, Associate Professor Dr. Yousif A. Khalid, Associate Professor Ir. Dr. Barkawi Bin Sahari and Associate Professor Dr. Abdel Magid Hamouda; for giving their greatest support and encouragement throughout the course of this project study. With their constant advice and guidance, this study was completed in a smooth and successful manner.

I also attribute my effort to all related parties, for their kind cooperation in providing me the valuable information concerning with my project and help me in one or another way during the project progress.

Last but not least, I would like to thank my family and friends for their moral supports and encouragements that motivate me to relentless strive to succeed.

I certify that an Examination Committee met on 9th September 2002 to conduct the final examination of Chan Chee Leong on his Master of Science thesis entitled “Experimental and Finite Element Analyses of Corrugated Web Steel Beams Subjected to Bending Loads” in accordance Universiti Pertanian Malaysia (Higher Degree) Act 1980 and Universiti Pertanian Malaysia (Higher Degree) Regulations 1981. The committee recommends that the candidate be awarded the relevant degree. Members of the Examination Committee are as follows:

WONG SHAW VOON, Ph.D.

Faculty of Engineering,
Universiti Putra Malaysia
(Chairman)

YOUSIF ABDULLAH KHALID, Ph.D.


Associate Professor,
Faculty of Engineering
Universiti Putra Malaysia
(Member)

IR. BARKAWI BIN SAHARI, Ph.D.

Associate Professor,
Faculty of Engineering
Universiti Putra Malaysia
(Member)

ABDEL MAGID S. HAMOUDA, Ph.D.

Associate Professor,
Faculty of Engineering
Universiti Putra Malaysia
(Member)


SHAMSHER MOHAMAD RAMADILI, Ph.D.
Professor/Deputy Dean
School of Graduate Studies,
Universiti Putra Malaysia

Date: 15 OCT 2002

This thesis submitted to the Senate of Universiti Putra Malaysia has been accepted as fulfilment of the requirements for the degree of Master of Science. The members of the Supervisory Committee are as follows:

YOUSIF ABDULLAH KHALID, Ph.D.

Associate Professor,
Faculty of Engineering
Universiti Putra Malaysia
(Chairman)

IR. BARKAWI BIN SAHARI, Ph.D.

Associate Professor,
Faculty of Engineering
Universiti Putra Malaysia
(Member)

ABDEL MAGID S. HAMOUDA, Ph.D.

Associate Professor,
Faculty of Engineering
Universiti Putra Malaysia
(Member)

AINI IDERIS, Ph.D.

Professor/Dean,
School of Graduate Studies,
Universiti Putra Malaysia

Date:

DECLARATION

I hereby declare that the thesis is based on my original work except for quotations and citations which have been duly acknowledged. I also declare that it has not been previously or concurrently submitted for any other degree at UPM or other institutions.



CHAN CHEE LEONG

12 OCT. 2002

TABLE OF CONTENTS

		Page
ABSTRACT		ii
ABSTRAK		iv
ACKNOWLEDGEMENTS		vi
APPROVAL SHEETS		vii
DECLARATION FORM		ix
LIST OF TABLES		xii
LIST OF FIGURES		xiv
LIST OF ABBREVIATIONS		xxi
CHAPTER		
1	INTRODUCTION	1
	1.1 Types of Structural Beams	1
	1.2 Ordinary I-Section Beams	1
	1.3 Corrugated Web Beams	2
	1.4 Manufacturing Process of the Corrugated Web Beams	3
	1.5 Objectives	4
	1.6 Thesis Layout	4
2	LITERATURE REVIEW	6
	2.1 Beam Description	6
	2.2 Investigation of Ordinary I-Section Beam	9
	2.3 Beams With Stiffeners	27
	2.4 Beams With Corrugated Web	34
	2.5 Failure Modes	55
	2.6 Finite Element Method (FEM)	58
	2.6.1 FEM Application and Methods	58
	2.6.2 Thick Shell Elements	63
	2.6.3 Stress Potential Definition	65
	2.7 Summary	67
3	METHODOLOGY	68
	3.1 Introduction	68
	3.2 Method	68
	3.3 Experimental Works	70
	3.3.1 Selecting Models Dimensions and Material	70
	3.3.2 Material Tensile Testing	72
	3.3.3 Specimens Fabrication	73
	3.3.4 Test Rig Fabrication	74
	3.3.5 Experimental Set-Up and Test Procedures	75
	3.3.6 Dimensional Measurement	77
	3.4 Analytical Works	78
	3.4.1 Pre-Processing	81
	3.4.1.1 Feature Definition and Model Creation	81

3.4.1.2	Element Selection and Mesh Generation	82
3.4.1.3	Material and Geometry Properties	87
3.4.1.4	Boundary Conditions and Constraints	91
3.4.1.5	Load Simulation	94
3.4.2	Finite Element Solver	95
3.4.3	Post-Processing	96
3.5	Summary	96
4	RESULTS	98
4.1	Experimental Results	98
4.1.1	Material Properties Tests	98
4.1.2	Three-Point Bending Tests	102
4.2	Finite Element Analysis Results	109
4.2.1	Ordinary I-Section Beam (Plane Web)	112
4.2.2	Welded I-Section Beam (Plane Web)	115
4.2.3	Horizontal-Corrugated Web Beam (HC1Rx and HC2Rx)	121
4.2.4	Vertical-Corrugated Web Beam (VCRx)	130
4.3	Comparing the Finite Element Analysis (FEA) Results for the Three Web Shapes	138
4.4	Comparing Ixx Values Obtained from the Experimental Tests, the Finite Element Analyses and the Theoretical Results	145
4.5	Comparison Between the Experimental Results and the Finite Element Analysis Results (FEA)	147
4.6	Summary	152
5	DISCUSSION	154
6	CONCLUSIONS AND RECOMMENDATIONS	163
	REFERENCES	166
	APPENDICES	170
	BIODATA OF THE AUTHOR	197

LIST OF TABLES

Table	Page
3.1	70
3.2	80
3.3	84
3.4	87
3.5	88
3.6	92
3.7	93
4.1	102
4.2	116
4.3	122
4.4	131
4.5	139
4.6	140
4.7	142
4.8	143
4.9	144
4.10	145
4.11	146

4.12	Comparison between $I_{xx}(FEA)$ and $I_{xx}(THEORY)$ using elastic bending equation.	147
4.13	Comparison of yield loads between the experimental and finite element analysis results.	148
5.1	Comparison between $I_{xx}(FEA)$ and $I_{xx}(THEORY)$ for various length.	161

LIST OF FIGURES

Figure		Page
2.1	Parameters for beams with (a) flat web (b) trapezoidal corrugated web (c) wholly corrugated web.	8
2.2	Experimental setup.	9
2.3	(a) I-section dimensions and sectorial coordinate ω , (b) and (c) stress (σ) diagram in partly plastic cross section in two cases (d) attainment of full plasticity.	10
2.4	Loading condition (a) and load-moment diagrams.	12
2.5	Braced and unbraced beams under eccentric loading.	13
2.6	Variations of in-plane central deflection with dimensionless bending moment for centrally braced beams (torsion free).	14
2.7	Variations of central twist rotation with dimensionless torque for unbraced beams.	14
2.8	m - v curves for I-section beam (accounted flange portion).	19
2.9	m - v curves for I-section beam (discarded flange portion).	20
2.10	Influence of point of load application.	21
2.11	Elastic beam with central torsional restraint. (a) Beam and restraints (b) First mode buckling shape ϕ ($\alpha_{RZ}=0$) (c) Second mode of buckling shape ϕ ($\alpha_{RZ}>\alpha_{RZL}$) (d) Axis system.	23
2.12	Suspended beam geometry.	26
2.13	(a) Beam with web stiffeners and batten plates (b) Specimens in experiment.	28
2.14	Correlation between M_{ex}/M_o and u or v .	29
2.15	Warping stiffening device of box type.	31
2.16	(a) Specimen with T-stiffeners (b) Specimen with angle-stiffener.	32
2.17	Load-deflection curves for MT1-MT5 specimens.	32
2.18	Cyclic loading sequence	33
2.19	Hysteretic load-deflection curve for specimen with shorter stiffener.	34

2.20	(a) Depth tapered beam (b) castellated beam.	35
2.21	Finite element model of corrugated web beams under shear load.	35
2.22	(a), (b) and (c) Local buckling on specimens with different corrugation configurations (d) Global buckling.	37
2.23	P- δ curves for various geometric parameters of trapezoidal corrugation.	38
2.24	Character of buckling modes (a) local buckling (b) zonal buckling (c) global buckling.	39
2.25	Corrugated web under pure shear.	40
2.26	Web deformation for various corrugation profiles under bending loads.	41
2.27	Membrane and bending stresses along x-axis.	41
2.28	Membrane and bending stresses along y-axis.	42
2.29	Cross section of test specimens.	43
2.30	Equivalent mechanical element.	44
2.31	Locations of applied load.	46
2.32	Interaction curves between bending and patch loading.	47
2.33	Interaction curves between shear and patch loading.	47
2.34	Load-deflection relations for different elastic-plastic models.	49
2.35	(a) Three loading positions (b) Load-deflection relations with different loading positions.	49
2.36	Load-deflection relations with different distribution of load applied at the flat part.	50
2.37	Load-deflection relations with various corrugation angles α .	50
2.38	Load-deflection relations with various web thickness t_w .	51
2.39	Load-deflection relations with various flange thickness t_f .	51
2.40	(a) The working principle of tooth rolls (b) Envelope of the family of curves (c) Flank profile of the tooth top.	54

2.41	Bending failure.	56
2.42	Flange buckling.	56
2.43	Web buckling and web bearing failures.	56
2.44	(a) Shear failure (b) Shear buckling.	57
2.45	Lateral torsion buckling.	57
2.46	Perforated thick plate modelled with the TTF6 elements.	59
2.47	Nonlinear load-displacement iteration based on Newton-Raphson method.	60
2.48	General type of elements.	60
2.49	Six meshes for convergence study for trapezoidal corrugated web.	61
2.50	Load-deflection relations obtained using different meshes for trapezoidal corrugated web beams.	62
2.51	Load-deflection relations obtained using different number of integration points through element thickness for trapezoidal corrugated web beams.	62
2.52	Hardening curve definition (a) Hardening gradient (b) Effective plastic strain (c) Effective total strain.	66
3.1	Methodology flow chart.	69
3.2	Geometry of the models tested experimentally.	71
3.3	Locations of tensile specimens cut from the ordinary flat web beam.	72
3.4	Tensile specimen dimensions and cross section at the gauge length (a) flat specimen (b) pipe.	73
3.5	Detail dimensions of experimental test rig.	75
3.6	Experimental set-up.	76
3.7	TUTOR inspection page.	78
3.8	Main stages of an analysis.	81
3.9	Quadrilateral thick shell elements.	83
3.10	Geometry features and meshes for OPW and WPWx models.	85

3.11	Geometry features and meshes for HC1Rx models.	85
3.12	Geometry features and meshes for HC2Rx models.	86
3.13	Geometry features and meshes for VCRx models.	86
3.14	Hardening curve for material M1.	89
3.15	Hardening curve for material M2.	89
3.16	Hardening curve for material M3.	90
3.17	Boundary conditions for half model.	91
3.18	Boundary conditions for full model.	92
3.19	Load simulation for half model.	94
3.20	Load simulation for full model (mainly VCRx models)	95
4.1	Tensile test results for specimens collected from web part of an I-beam.	99
4.2	Tensile test results for specimens collected from top flange of an I-beam.	100
4.3	Tensile test results for specimens collected from bottom flange of an I-beam.	100
4.4	Tensile test results for flat bars.	101
4.5	Tensile test results for pipes.	101
4.6	Experimental results for OPW type.	103
4.7	Experimental results for WPW1 type.	103
4.8	Experimental results for HC1R1-1 type.	104
4.9	Experimental results for HC2R1-1 type.	104
4.10	Experimental results for VCR3-1 type.	105
4.11	OPW-1 specimen at 13 mm machine crosshead displacement.	106
4.12	WPW1-1 specimen at 15 mm machine crosshead displacement.	107
4.13	HC1R1-1-1 specimen at 16 mm machine crosshead displacement.	107
4.14	HC2R1-1-1 specimen at 18 mm machine crosshead displacement.	108

4.15	VCR3-1-1 specimen at 15 mm machine crosshead displacement.	108
4.16	Web distance across the span.	111
4.17	Finite element analysis results for OPW model.	112
4.18	Deformed mesh of OPW model (in the plastic state) at 5 mm maximum displacement on the top flange.	113
4.19	Distribution of stress component in the z-direction for the OPW model at 25 kN load (3.125 kNm moment at the half span).	113
4.20	σ_{zz} in the web at section A-A on the OPW model (at 25 kN load).	114
4.21	σ_{zz} in the flanges at section A-A on the OPW model (at 25 kN load).	114
4.22	Deformed mesh of WPW7 model (in the plastic state) at 5 mm maximum displacement on the top flange.	117
4.23	Distribution of stress component in the z-direction for the WPW7 model at 25 kN load (3.375 kNm moment at the half span).	117
4.24	σ_{zz} in the web at section A-A on the WPW7 model (at 25 kN load).	118
4.25	σ_{zz} in the flanges at section A-A on the WPW7 model (at 25 kN load).	118
4.26	Finite element analysis results for WPWx models with different flanges materials.	120
4.27	Finite element analysis results for WPWx models with different web materials.	120
4.28	Finite element analysis results for HC1R1-x models with different web material.	122
4.29	Finite element analysis results for HC1R2-x models with different web material.	123
4.30	Finite element analysis results for HC1R3-x models with different web material.	123
4.31	Load-displacement curves for HC1Rx-3 models with different corrugation radius (L=540mm).	124
4.32	Load-displacement curves for HC2Rx-1 models with different corrugation radius (L=500mm).	124

4.33	Load-displacement curves for HC2Rx-2 models with different corrugation radius (L=540mm).	125
4.34	Deformed mesh of HC1R1-3 model (in the plastic state) at 5 mm maximum displacement on the top flange.	125
4.35	Deformed mesh of HC2R1-2 model (in the plastic state) at 5 mm maximum displacement on the top flange.	126
4.36	Distribution of stress component in the z-direction for the HC1R1-3 model at 25 kN load (3.375 kNm moment at the half span).	126
4.37	Distribution of stress component in the z-direction for the HC2R1-2 model at 25 kN load (3.375 kNm moment at the half span).	127
4.38	σ_{zz} in the web at section A-A on the HC1R1-3 model (at 25 kN load).	127
4.39	σ_{zz} in the flanges at section A-A on the HC1R1-3 model (at 25 kN load).	128
4.40	σ_{zz} in the web at section A-A on the HC2R1-2 model (at 25 kN load).	128
4.41	σ_{zz} in the flanges at section A-A on the HC2R1-2 model (at 25 kN load).	129
4.42	Deformed mesh of VCR3-2 model at 5 mm maximum displacement on the top flange.	132
4.43	Distribution of stress component in the z-direction for the VCR3-2 model at 25 kN load (3.375 kNm moment at the half span).	132
4.44	σ_{zz} in the web at section A-A on the VCR3-2 model (at 25 kN load).	133
4.45	σ_{zz} in the flanges at section A-A on the VCR3-2 model (at 25 kN load).	133
4.46	Load-displacement curves for VCRx models with different corrugation radius (L=540mm).	134
4.47	Finite element analysis results for VCR3-x models with different web thickness.	135
4.48	Finite element analysis results for VCR3-x models with different web and flanges materials.	135
4.49	Supports and loading position on the bottom and top flanges respectively for VCR3-6 model.	137

4.50	Deformed mesh of VCR3-6 model at 6 mm maximum displacement on the top flange.	137
4.51	Comparison of F_y values between the corrugated web and plane web (WPW7) models with the same geometry dimensions and material properties.	140
4.52	Comparison of F_y/w ratio between the corrugated web and plane web (WPW7) models with the same geometry dimensions and material properties.	141
4.53	Comparison of S values between the vertical-corrugated web and plane web (WPW7) models with the same geometry dimensions and material properties.	144
4.54	Comparison between experimental tests and finite element analysis results for OPW model.	148
4.55	Comparison between experimental tests and finite element analysis results for WPW1 model.	149
4.56	Comparison between experimental tests and finite element analysis results for HC1R1-1 model.	149
4.57	Comparison between experimental tests and finite element analysis results for HC2R1-1 model.	150
4.58	Comparison between experimental tests and finite element analysis results for VCR3-1 model.	150
4.59	Comparison of top flange's deformation for OPW model obtained from CMM measurements and finite element analysis.	151
4.60	Local vertical flange buckling and web rippling in specimen OPW-1.	152
5.1	Corrugation parameters for VCRx models.	159
5.2	$W\lambda$ against H/b_f for all VCRx models.	159
B1.1	Determination of slope from load-machine crosshead displacement curve for specimen OPW1.	176

LIST OF ABBREVIATIONS

A_{xy}	Area of cross section in the xy plane
A_{zx}	Area of cross section in the zx plane
b_f	Width of flange
d	Depth of beam
d_m	Mean diameter of corrugated web
ep	Effective plastic strain
e	Strain
E	Modulus of Elasticity
F	Load
F_U	Ultimate load
F_Y	Yield load
H	Corrugation amplitude
I_{xx}	Second moment of area with respect to x-axis
$I_{xx(EXP)}$	Second moment of area with respect to x-axis obtained from experimental tests
$I_{xx(FEA)}$	Second moment of area with respect to x-axis obtained from finite element analyses
$I_{xx(THEORY)}$	Second moment of area with respect to x-axis obtained from theoretical equations
L	Beam length/span
M	Bending moment
M_ω	Moment measured in sectorial coordinate- ω
M_Y	Yield moment
M_U	Ultimate moment
P	Load applied on compression flange
p	Loading position on vertically corrugated web beam
r	Corrugation radius
r_i	Inner radius/minor radius of arc
r_o	Outer radius/major radius of arc
S	Elastic section modulus
t	Web thickness at cross section
t_f	Flange thickness
t_w	Web thickness
V	Volume
W	Specific weight
w	Weight per unit length
ω	Sectorial coordinate
λ	Cycle length
σ	Direct stress
σ_{max}	Maximum bending stress
σ_U	Ultimate strength
σ_y	Yield stress
δ	Displacement
AISC	American Institute of Steel Construction
ASD	Allowable Stress Design
LRFD	Load and Resistance Factor Design

CHAPTER 1

INTRODUCTION

1.1 Types of Structural Beams

Structural beams are common building materials and normally made of steel. In order to simplify the design and construction process, all characteristics or geometries of the beams are specified in accordance to the approved standards such as the American Iron and Steel Institute (AISI), American Society for Testing and Materials (ASTM) and British Standards (BS). The common commercial structural shapes available are hot-rolled cross sections (such as wide-flange, channels and angles), pipe and hollow structural sections (HSS).

1.2 Ordinary I-Section Beams

The I-section beam or H-pile plays an important role in the construction industry for building of structures such as bridges, water tank supports and towers. Its uniqueness in shape, which consists of two parallel flanges and a slender web, creates more versatility to suit most working environments. It is commonly made from steel materials through hot or cold form-rolling process of steel bloom.

In line with the development of construction and manufacturing industries, higher requirement and quality standard sets for these beams is essential. Designers and manufacturers have used numerous ways in producing an ideal beam that is safer, reliable and economical in materials and production cost. These include modifying

the ordinary shape of the beam and optimising the sizes to suit the demand. For instance, the hollow flange beam (HFB) was introduced in replacing the conventional beam type in certain application and usage of external or internal stiffeners to produce stronger structures.

However, these alternatives seem to be more expensive and added extra weight to the structure, making it impractical when delivery of materials is concerned. Some even appear to have contributed insignificant improvement to the beam's performance in comparison to the ordinary one.

1.3 Corrugated Web Beams

The beams with wholly corrugated web (WCW) has been introduced and used in building and construction industries. It could economise on materials and yet stronger in strength than the conventional beams. However, the information relevant to its mechanical behaviour and limitation in practice is inadequate. The effects of the corrugation parameters and beams' dimensions to the bending performance are still scarce.

Recently, as its application grew in many industries, especially construction, these parameters have been the main research subjects. The preliminary studies being carried out on such beams were mainly concentrated on the trapezoidal corrugation in the vertical direction. With reference to the available data from both experimental and analytical works, the corrugation has contributed equal stability to the web

regardless of the materials thickness. This applies for the major loading modes like bending, shearing and buckling.

However, manufacturing of these beams is difficult and bounded by the limitation and tolerances of the process, which would limit its usage in practice. This is especially true when standardization of sizes is concerned.

1.4 Manufacturing Process of the Corrugated Web Beams

The general shape-rolling process adopted for the ordinary beams with flat web can not be implemented for the trapezoidal corrugated web type. At present, the web is welded continuously at the joints on the two flanges that produce an I-cross section. Nevertheless, strong joints could hardly be produced for beams with thinner web, even by the use of state of art welding technology that could possibly do the job. Higher cost will certainly be incurred that make it impractical especially for a longer span.

Thus, the curve wave-like corrugation was introduced to substitute the trapezoidal corrugation, as it seems more suitable to be manufactured. However, to date, the same welding method is being used in producing this corrugation shape where the hot rolled beam of the similar type has yet been produced by any manufacturer. Although, few successful in laboratory trials have been seen in some research works, but the design of the roll process and tools are not fully addressed. The design requirements of the roll tool for corrugated web beams are outlined as follow.